



ผลของโครงสร้างท่อนาโนไทเทเนียมไดออกไซด์ต่อปฏิกิริยาโฟโตแคตะไลติก ที่เตรียมโดยการแอโนไดเซชันจากฟิล์มไทเทเนียม

Effect of the Structure of a TiO₂ Nanotube Arrays on Photocatalytic Activity

Prepared by Anodization from Sputtered Ti Film

วัชระ สุภาพ¹, ฉันทนา เอี่ยมพานิกิจ² และ กมล เอี่ยมพานิกิจ^{1*}

Watchara Suphap¹, Chantana Aiempnanikit², and Kamon Aiempnanikit^{1*}

¹ ภาควิชาฟิสิกส์ คณะวิทยาศาสตร์และเทคโนโลยี มหาวิทยาลัยธรรมศาสตร์

² สาขาวิชาฟิสิกส์ คณะวิทยาศาสตร์และเทคโนโลยี มหาวิทยาลัยเทคโนโลยีราชมงคลธัญบุรี

¹ Department of Physics, Faculty of Science and Technology, Thammasat University

² Division of Physics, Faculty of Science and Technology, Rajamangala University of Technology Thanyaburi

Received : 15 June 2021

Revised : 23 September 2021

Accepted : 10 October 2021

บทคัดย่อ

ท่อนาโนไทเทเนียมไดออกไซด์ถูกสังเคราะห์ผ่านกระบวนการแอโนไดเซชันจากฟิล์มไทเทเนียมที่เคลือบบนกระจกอินเดียมทินออกไซด์โดยเทคนิคดีซีแมกนีตรอนสปัตเตอร์ ท่อนาโนไทเทเนียมไดออกไซด์ถูกสร้างขึ้นโดยใช้ศักย์ไฟฟ้า 30 โวลต์ และสารละลายอิเล็กโทรไลต์ที่ประกอบด้วยแอมโมเนียมฟลูออไรด์ เอทิลีนไกลคอล และน้ำปราศจากไอออน 1 – 3 vol% โครงสร้างและสัณฐานวิทยาของท่อนาโนไทเทเนียมไดออกไซด์จะถูกตรวจสอบด้วยเครื่องเอ็กซ์เรย์ดิฟแฟกซ์โทรมิเตอร์ และกล้องจุลทรรศน์อิเล็กตรอนแบบส่องกราดชนิดฟิวซิซึมชัน ตามลำดับ ผลที่ได้แสดงให้เห็นว่าค่าเฉลี่ยของเส้นผ่านศูนย์กลางท่อนาโนไทเทเนียมไดออกไซด์ที่เงื่อนไขปริมาณน้ำปราศจากไอออน 1 2 และ 3 vol% จะมีค่า 45.63 55.30 และ 65.32 นาโนเมตรตามลำดับ และขนาดผลึกของท่อนาโนไทเทเนียมไดออกไซด์หลังอบสามารถคำนวณได้จากสมการของเชอร์เรอร์ ได้ขนาดผลึกระนาบ (004) เพิ่มขึ้นจาก 24.34 เป็น 29.53 และ 30.61 นาโนเมตร เมื่อปริมาณน้ำปราศจากไอออนเพิ่มขึ้น ในงานวิจัยพบว่าท่อนาโนไทเทเนียมไดออกไซด์ที่เตรียมด้วยปริมาณน้ำปราศจากไอออน 3 vol% จะมีขนาดผลึกและเป็นระเบียบสูงสุด ซึ่งโครงสร้างและขนาดของท่อเป็นปัจจัยที่สำคัญที่ส่งผลกระทบต่อปฏิกิริยาโฟโตแคตะไลติก โดยท่อนาโนไทเทเนียมไดออกไซด์ที่ได้จะถูกนำไปทดสอบการย่อยสลายสารละลายเมทิลีนบลูภายใต้การฉายรังสีที่เวลาต่างๆ พบว่าท่อนาโนไทเทเนียมไดออกไซด์ที่เงื่อนไขที่สูงสุดสำหรับปฏิกิริยาโฟโตแคตะไลติกคือปริมาณน้ำปราศจากไอออน 3 vol% เนื่องจากพื้นที่ผิวและขนาดผลึกที่เพิ่มขึ้น

คำสำคัญ : ท่อนาโนไทเทเนียมไดออกไซด์, ปฏิกิริยาโฟโตแคตะไลติก, สปัตเตอร์, แอโนไดเซชัน



Abstract

In this research, titanium dioxide nanotubes (TNTs) were synthesized via an anodization process from titanium (Ti) film sputtered on indium tin oxide (ITO) glass by a DC magnetron sputtering technique. The TNTs were fabricated by using potential at 30 V and electrolyte solution consisted of ammonium fluoride (NH_4F), ethylene glycol (EG), and deionized water at 1-3 vol%. The crystal and surface morphology of TNTs were characterized by an X-Ray Diffractometer (XRD) and Field Emission Scanning Electron Microscopy (FE-SEM), respectively. The results showed that the average diameters of TNTs with deionized water of 1, 2, and 3 vol% were 45.63, 55.30, and 65.32 nm, respectively. The crystallite size of the annealed TNTs at (004) plane were calculated from the Scherrer equation, which increased from 24.34 nm to 29.53 and 30.61 nm with increasing percent by volume of deionized water. It was found that TNTs prepared with deionized water at 3 vol% showed the highest crystallite size and uniform diameter. The crystal structure and tubular size of TNTs are important factors that affect the photocatalytic reaction. The TNTs were tested for the degradation of methylene blue in an aqueous solution under various UV irradiation times. The best TNTs condition for photocatalytic activity was anodized with deionized water at 3 vol% due to an increase surface area and crystallite size.

Keywords : titanium dioxide nanotubes ; photocatalytic reaction ; sputtering ; anodization



Introduction

Currently, titanium dioxide (TiO_2) films are given significant attention for use in applications such as sensors (Alba *et al.*, 2020; Fan *et al.*, 2021), catalysts (Matus *et al.*, 2018; Thomas *et al.*, 2020; Perillo *et al.*, 2021), electrochromic (Zhang *et al.*, 2020; Lee *et al.*, 2021), and solar cells (Nguyen *et al.*, 2020; Chen *et al.*, 2021; Gnida *et al.*, 2021). TiO_2 films can be synthesized in a nanoscale structure, such as nanotubes, nanoparticles, and nanowires, etc. However, the structure of TNTs also shows suitability for use in photocatalytic reactions, because the structure enhances the active surface area, enabling the electrons to move rapidly. TNTs can be synthesized by anodization from Ti foil (Naduvath *et al.*, 2015), Ti plate (Vera *et al.*, 2017) and Ti film (Szkoda *et al.*, 2016) in an electrolyte solution are comprised of fluoride. Gong and co-worker (Gong *et al.*, 2001) generated TNTs by anodizing a Ti foil in hydrofluoric acid solution. They reported that TNTs had limited thickness. While TNTs were synthesized in an electrolyte solution containing hydrofluoric acid (HF), ammonium fluoride (NH_4F) or sodium fluoride (NaF), and ethylene glycol (EG) or glycerol (GR) resulted in the increased thickness of TNTs at higher than 2 μm (Richter *et al.*, 2010; Chen *et al.*, 2013; Wang *et al.*, 2015; Gao *et al.*, 2016). TNTs can be up to 10 μm in length, but those produced from Ti foil have limited applications because TNTs can be broken and separated from the Ti foil. Therefore, the current research interest is the synthesis of TNTs on substrate materials such as glass and silicon. There are many methods for the synthesis of TNTs on substrates. One method is anodization from Ti deposited on a substrate. The deposition of Ti film can be achieved using the sputtering technique (Kaewwongsa *et al.*, 2017). The sputtering technique is advantageous in terms of the good adhesion of the film on the substrate due to this technique producing the high energy of an adatom deposited on a substrate via the transferring of momentum and energy from the argon ions. Usually, TNTs are synthesized by using Ti film deposited on a silicon substrate through direct current (DC) magnetron sputtering (Yang *et al.*, 2008) and Ti film deposited on indium tin oxides (ITO) glass using radio frequency (RF) sputtering (Lim *et al.*, 2011), which is achieved at a substrate temperature of 500 °C. The substrate must be heated before deposition due to enhancement of dense Ti film. Moreover, anodization processes were observed such as the type of electrolytes (Lim *et al.*, 2011; Szkoda *et al.*, 2016) concentration or amount of solution (Regonini *et al.*, 2012; Szkoda *et al.*, 2016), and electrical potential used in anodization (Regonini *et al.*, 2012). These parameters affect the structural and optical properties of TNTs.

Photocatalytic activity is an interesting property of TNTs because light can be absorbed and electrons exchange well, in addition to being resistant to chemical reactions. The TNTs were fabricated by an anodic oxidation process and investigated for the effects of the structure on photocatalytic activity. Annealed TNTs at temperature of 500 °C for 1 h exhibited the most photodegradation of methylene blue in 2,3-dichlorophenol in an aqueous



solution under UV light radiation (Liang *et al.*, 2009). The effects of anodization duration on morphology and photocatalytic activity showed that the best photodegradation rate (k) was about 0.0104 min^{-1} (Suhaimy *et al.*, 2018).

Although there have been many reports over the years concerning the variables that affect photocatalytic reactions, there have been few reports focused on the effects of electrolyte solution and annealing on the anodization process of photocatalytic properties. Additionally, reports concerning TNTs synthesized from sputtered Ti film without substrate heating have been scarce. Therefore, this work was interested in studying Ti film deposition on ITO glass without external heating by DC magnetron sputtering and electrolyte ratio in the anodization process. The TNTs were tested for photocatalytic activity using various UV irradiation times, after which the morphology, crystal structure, and optical properties of TNTs on photocatalytic activity were discussed.

Methods

Ti and TNTs preparations

ITO glass ($1 \times 2.5 \text{ cm}^2$) was ultrasonically cleaned in acetone, ethanol, and deionized water for 15 min and then dried in air. The Ti film was deposited onto cleaned ITO glass using the DC magnetron sputtering technique from 99.99% pure Ti target (Kurt J. Lesker). The sputtering power of 200 W was applied at a deposition time of 16.40 min, as shown in Table 1. After that, TNTs were synthesized via anodization in a dual-electrode reaction chamber. Lead (Pb) sheet and Ti coated on ITO glass were used as cathode and anode, respectively. Two electrodes were soaked in electrolyte containing NH_4F of 0.6 wt%, deionized water of 1-3 vol% (TNTsx where x is deionized water vol%), and ethylene glycol of 97-99 vol% which used potential at 30 V for 2 h, as summarized in Table 2. All TNTs were subsequently annealed in a furnace at a temperature of 450°C for 1 h (a-TNTsx where x is deionized water vol%).

Film characterization

The structure and surface morphology of TNTs were characterized with an X-Ray Diffractometer (XRD, Bruker, D2 Phaser) at 30 kV and 10 mA ($\text{CuK}\alpha$ with $\lambda = 1.5406 \text{ \AA}$) and Field Emission Scanning Electron Microscopy (FE-SEM, JEOL 6060), respectively. The optical property of TNTs was determined by UV-Visible Spectrophotometer (GENESYS10S). Methylene blue in an aqueous solution was prepared at a concentration of 0.01 to 0.05 mM to find the calibration curve. The photocatalytic activity of TNTs was investigated by the degradation of methylene blue in an aqueous solution at a concentration of 0.05 mM. A photoreaction was performance within a UV box consisting of a UV light source (SANTORY, Blacklight lamp, F10T8BL 20 W, Japan). The distance between the top surface of



the solution and lamp was about 10 cm, while irradiation time was 50, 100, 150, and 200 min. After irradiation, the absorbance of methylene blue (MB) in an aqueous solution was measured by a UV-visible spectrometer. The absorbance data of methylene blue with different catalysts of TNTs were analyzed to impose the degradation rate of methylene blue.

Table 1 Conditions for the sputtering technique

Parameters	Conditions
Target	Titanium
Base pressure	5×10^{-5} mbar
Sputtering power	200 W
Flow rate of argon gas	15 sccm
Substrate	ITO glass
Deposition time	16.40 min

Table 2 Conditions of the anodization process.

Samples	Electrolyte			Voltage (V)	Duration (h)
	NH ₄ F (wt%)	Ethylene glycol (vol%)	deionized water (vol%)		
TNTs1	0.6	99	1	30	2
TNTs2	0.6	98	2	30	2
TNTs3	0.6	97	3	30	2

Results

Morphology and structure of Ti film

The morphology of Ti film deposited on 100 nm thickness ITO coated glass substrates by using DC magnetron sputtering technique is shown in Figure 1. The results indicated that the Ti film had a large grain size about 275 nm with a columnar structure. In this study, we used high sputtering power at 200 W to prepare Ti film which effected on substrate self-heating, deposition rate and structure of Ti film (Lim *et al.*, 2011). Moreover, the thickness of Ti film around 0.835 μm , as shown in Fig. 1 (b), effected the TNTs after anodization (Lim *et al.*, 2011).

The Ti film was examined for crystal structure, as shown in Fig. 2. It was found that the Ti film exhibited crystal structure (PDF 01-086-2608) with diffraction peak of 2θ at 38° and 40° corresponding to the crystal plane of (002) and (101), respectively. It can be said that high sputtering power can be promoted with a film to have a crystalline structure, even without substrate heating.

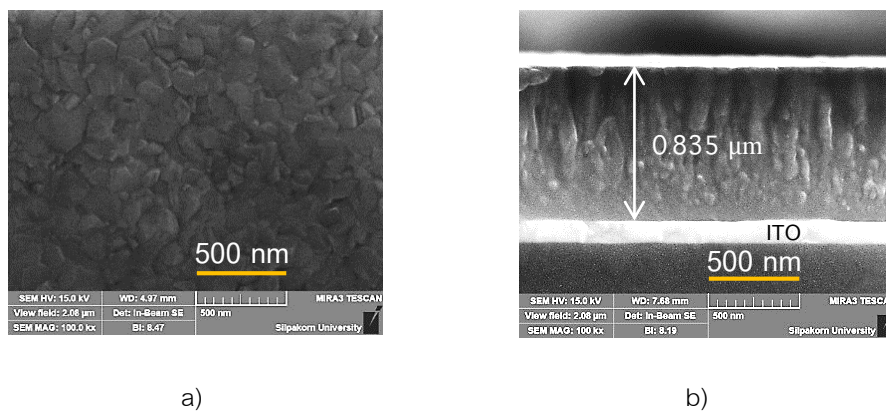


Figure 1 FE-SEM images of Ti film prepared by the dc magnetron sputtering technique: a) top view and b) cross-section view.

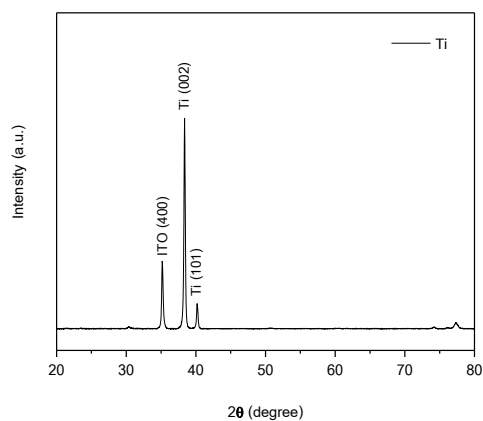


Figure 2 XRD pattern of Ti film prepared by the DC magnetron sputtering technique.

Morphology and structure of TNTs arrays

The variables of deionized water and EG in the electrolyte solution were used for the anodization process that affected the morphology of the TNTs arrays presented in Figure 3. We found that increasing the deionized water resulted in the increasing diameter and effected on the length of TNTs arrays. This result corresponded with previous research (Sreekantan *et al.*, 2009; Yang *et al.*, 2016; Simi *et al.*, 2017) due to the increase of hydrogen and oxygen ions.

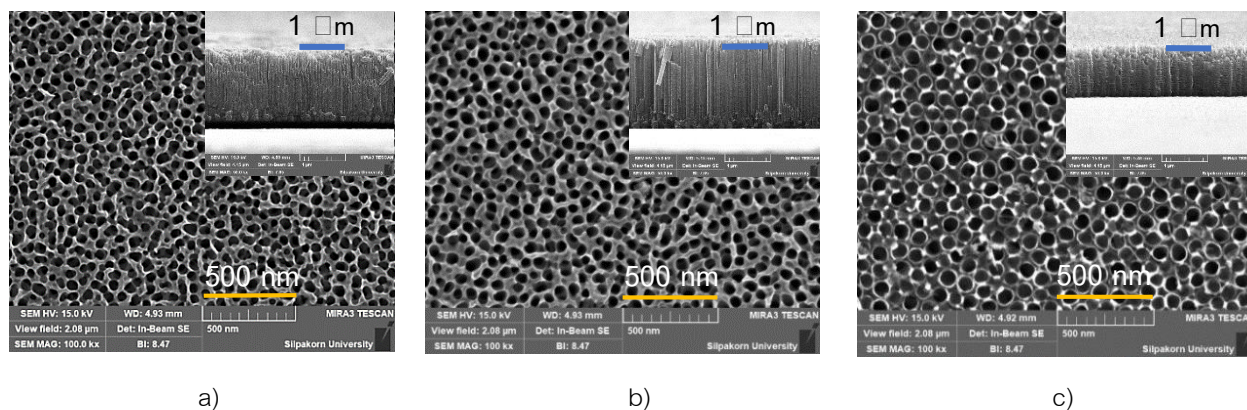


Figure 3 Top view and cross-sectional (insert) FE-SEM image of TNTs film prepared by anodization and deionized water of a) 1 vol%, b) 2 vol%, and c) 3 vol%.

The morphology of TNTs with varied deionized water at 1-3 vol% was analyzed with the diameter by which the technique distribution is presented in Fig. 4. We found that deionized water at 3 vol% had the smallest standard deviation of 7.087 and maximum average diameter of 65.32 nm. Deionized water at 1 and 2 vol% had standard deviations of 10.133 and 11.184, and average diameters of 45.63 nm and 55.30 nm, respectively. The data implies that deionized water at 3 vol% indicated the uniform diameter of the TNTs arrays. Moreover, the TNTs are clearly separated from each other. This results in a greater surface area both inside and outside the TNTs compared to other conditions.

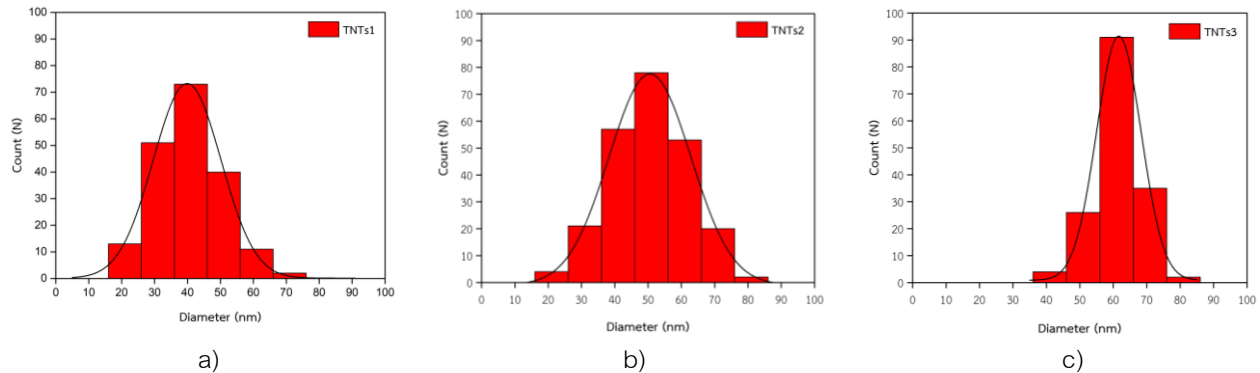


Figure 4 Distribution of diameters in TNTs arrays for deionized water at a) 1 vol%, b) 2 vol%, and c) 3 vol%.

XRD patterns of as-prepared and annealed TNTs arrays prepared with varied amounts of deionized water at 1-3 vol% are presented in Figure 5. The results showed that the as-prepared TNTs did not have the XRD peak shown to be amorphous, while the structure of annealed TNTs was the anatase phase of TiO_2 (PDF 03-065-5714). The crystal structure of TNTs exhibited that XRD diffraction peak of 2θ at 25.30° , 37.87° , 48.03° , and 53.98° of deionized water at 1 vol%, 25.28° , 37.93° , 48.37° , and 53.88° of deionized water at 2 vol%, and 25.28° , 37.80° , 48.05° , and 53.89° of deionized water at 3 vol% corresponded to the crystal planes of (101), (004), (200), and (105), respectively. We found that deionized water of 2 vol% in an electrolyte solution resulted in the highest crystallinity.

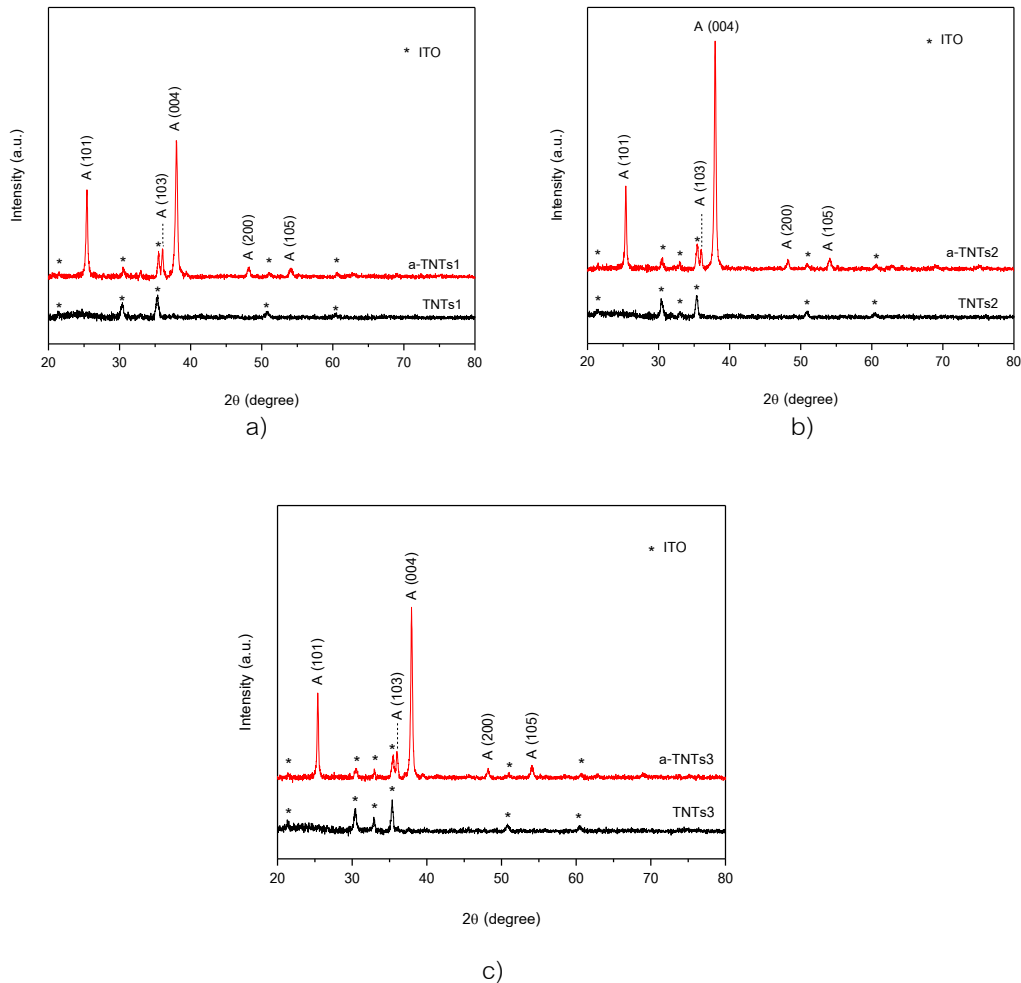


Figure 5 XRD pattern of both as-prepared and annealed TNTs arrays for deionized water at a) 1 vol%, b) 2 vol%, and c) 3 vol%.

The crystallite size of the annealed TNTs arrays was analyzed from the Scherrer equation (Yuan *et al.*, 2013). Average crystallite size at conditions of deionized water at 1, 2, and 3 vol% at (004) plane was 24.34, 29.53, and 30.61 nm, respectively.

Optical properties of TNTs arrays

The transmittance spectra of TNTs arrays for condition before and after annealing are shown in Figure 6. Varying deionized water amount significantly affected the transparency of TNTs film. The results showed that the transmittance spectra of TNTs arrays decreased when increasing deionized water. Moreover, annealed TNTs arrays exhibited lower transmittance than as-prepared under all conditions due to increasing oxygen vacancies formed during annealing (Lim *et al.*, 2011). The rapid decrease in transmittance at a wavelength range from 300 nm to 380 nm was the absorption edge of TiO_2 .

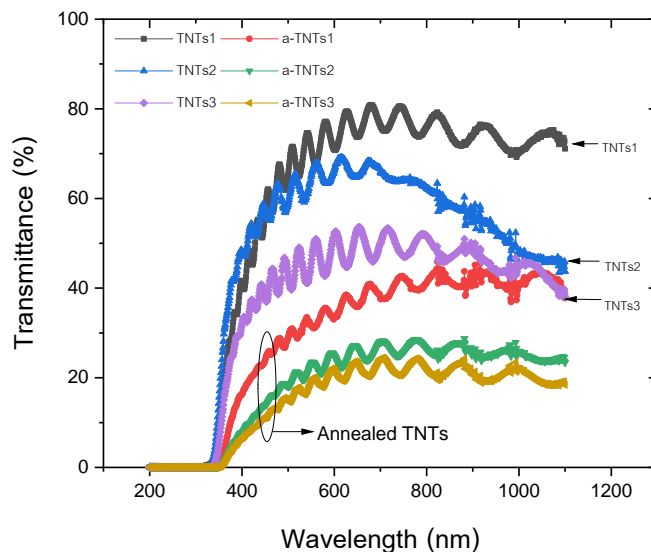


Figure 6 Transmittance spectra of annealed and as-prepared TNTs arrays.

Photocatalytic activity of TNTs arrays

The photocatalytic activity of TNTs arrays was measured by the degradation of MB in an aqueous solution under UV irradiation. The absorbance of the MB at concentrations of 0.01, 0.02, 0.03, 0.04, and 0.05 M was measured at a wavelength of 664 nm to create the calibration curve for analyzing the desired concentration, as presented in Figure 7. It was found that the relationship between the absorbance and concentration of MB obtained a linear curve corresponding to the Beer–Lambert Law (Swinehart, 1962) with the relationship as equation $y = 0.03411x$ and R^2 (Regression) = 0.99019.

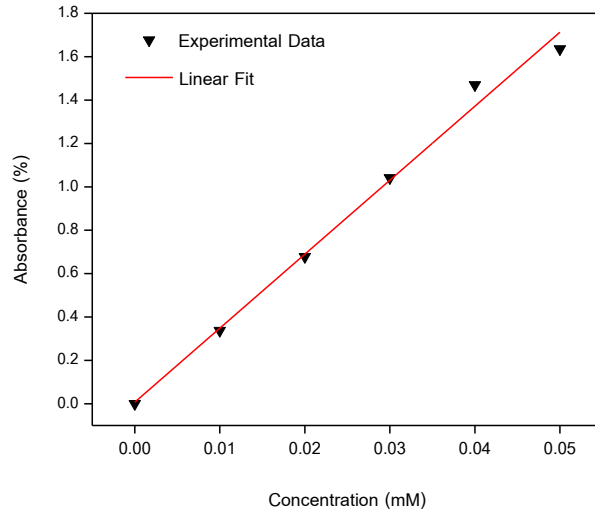


Figure 7 The calibration curve of MB in an aqueous solution.

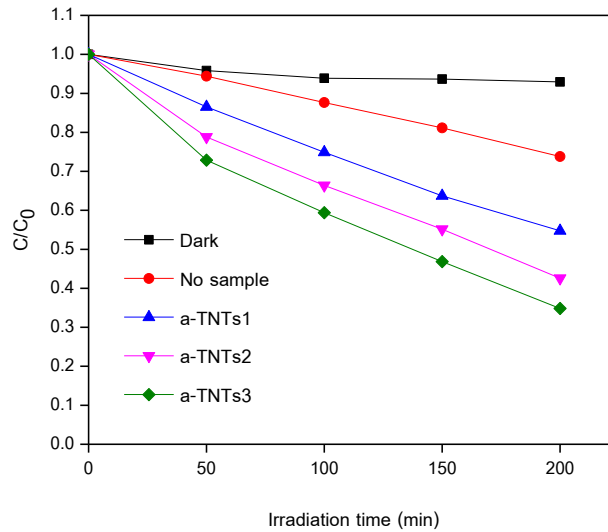


Figure 8 Relationship between C/C_0 and irradiation time of all annealed TNTs arrays.

Figure 8 shows the relationship between C/C_0 and reaction time, where C_0 is the initial concentration of MB and C is the concentration of MB after UV irradiation. It was found that the samples of MB in the dark and under UV irradiation were slightly decayed. The a-TNTs3 represented the highest photocatalytic activity, which corresponds



to the kinetics of decay of MB by plotting the graph between $\ln(C_0/C)$ and reaction time. We found that a first-order kinetic reaction for samples of dark, no sample, a-TNTs1, a-TNTs2, and a-TNTs3 corresponded to k values of 0.37×10^{-3} , 1.52×10^{-3} , 3.01×10^{-3} , 4.27×10^{-3} , and $5.27 \times 10^{-3} \text{ min}^{-1}$, respectively, as presented in Figure 9.

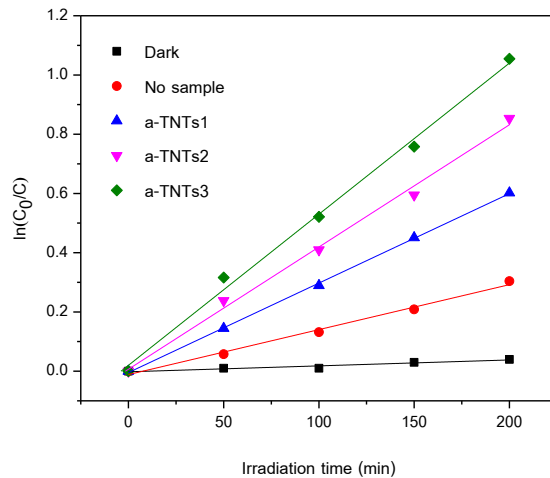


Figure 9 Plot $\ln(C_0/C)$ versus irradiation time of all annealed TNTs arrays.

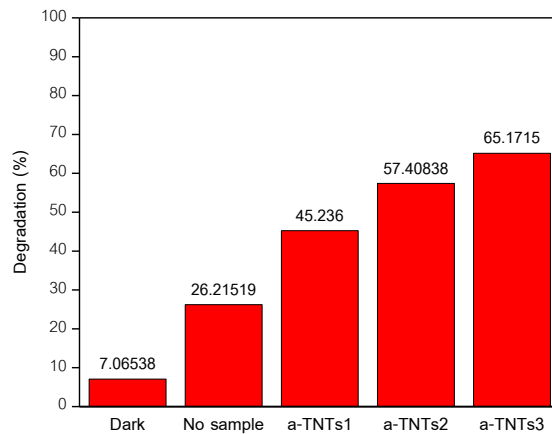


Figure 10 Percentage degradation of MB of all annealed TNTs arrays.

Figure 10 shows the degradation of MB at UV irradiation time for 200 min compared with all samples. It can be seen that the degradation of MB increased from 7.06 to 26.215, 45.236, 57.408, and 65.171% ,



corresponding with conditions of dark, no sample, a-TNTs1, a-TNTs2, and a-TNTs3, respectively. These results indicated that the TNTs exerted the degradation of MB as a function of increasing deionized water.

Discussion

The Ti film was deposited on ITO glass substrates using the DC magnetron sputtering technique without external heating. A sputtering power of 200 W was applied with a deposition time of 16.40 min, which resulted in the morphology of Ti film with columnar structure at a thickness of 0.835 μm . It was also shown that the crystal structure due to high sputter power caused substrate self-heating. Adatom at high energy deposited on the substrate enhanced the dense film arrangement of the columnar structure (Lv *et al.*, 2016). The TNTs were fabricated via an anodization process with varied deionized water amounts and EG in an electrolyte solution. The FE-SEM images of TNTs exhibited that an increase in deionized water resulted in the increasing diameter of TNTs arrays. TNTs with deionized water at 3 vol% clearly showed the separation of each nanotube. This is likely because deionized water enhanced the oxygen and hydrogen ions in the electrolyte solution, which affected the growth and etching rate of the TiO_2 layer (Srimuangmak *et al.*, 2011). Moreover, the XRD pattern of TNTs arrays indicated all samples of as-prepared were amorphous structure which transferred the crystal structure with the anatase phase after annealing. An annealing temperature of 450 °C for 1 h was sufficient energy to rearrange an atom in TNTs structure. Finally, the degradation of the MB solution was observed for the effect of TNTs structure. Increasing diameter size and separation of the nanotube structure to enhance the active surface area are important factors for photocatalytic activity (Hui *et al.*, 2007; Xu *et al.*, 2014). A large surface area can increase the absorption of MB and enable the trapping of electrons on the surface (Chen *et al.*, 2006). Additionally, increase absorption resulted in higher electron-hole pairs generation which enhanced photocatalytic properties (Ji *et al.*, 2017; Kang *et al.*, 2019). Therefore, the best efficiency of photocatalytic activity was annealed TNTs with anodization using deionized water at 3 vol%.

Conclusions

TNTs arrays were successfully prepared by anodization from titanium film sputtered on ITO glass using a DC magnetron sputtering technique without external heating. XRD confirmed that Ti film sputtered onto ITO glass without substrate heating can generate the crystal structure of Ti film with a columnar structure. The TNTs arrays were synthesized via the anodization process by using potential at 30 V and electrolyte solution composite of fixed NH_4F and various EG of 97-99 vol% as well as deionized water at 1-3 vol%. Increasing deionized water resulted in



the increasing diameter of TNTs arrays and showed separation of each nanotube with deionized water at 3 vol%. Annealing TNTs arrays at a temperature of 450 °C for 1 h promoted the anatase phase of the TiO₂ structure. The photocatalytic activity of TNTs arrays was investigated by the degradation of MB under various UV irradiation times. The a-TNTs3 showed the highest photocatalytic activity with degradation of 65.171%.

Acknowledgements

The authors would like to thank the Faculty of Science and Technology, Thammasat University and Division of Physics, Faculty of Science and Technology, Rajamangala University of Technology Thanyaburi for the provision of research facilities.

References

- Alba, A-H., Carlos, Z-I., Julio César, M-C., Kleider, Johnson, J-P. (2020). A study of the effect of morphology on the optical and electrical properties of TiO₂ nanotubes for gas sensing applications. *The European Physical Journal Applied Physics*, 90(3), 30102.
- Chen, Y.J., & Dionysiou, D.D. (2006). Correlation of structural properties and film thickness to photocatalytic activity of thick TiO₂ film coated on stainless steel. *Appl. Catal*, 69, 24-33.
- Chen, C., Li, F., Li, G., Tan, F., Li, S., & Ling, L. (2013). Double-sided transparent electrodes of TiO₂ nanotube arrays for highly efficient CdS quantum dot-sensitized photoelectrodes. *Journal of Materials Science*, 49 (4), 1868 –1874.
- Chen, C.-N., Wang, Y.-W., Ho, Y.-R., Chang, C.-M., Huang, W.-C., & Huang, J.-J. (2021). Liquid phase deposition/anodizing of TiO₂ nanotube working electrode for dye-sensitized solar cells. *Materials Science in Semiconductor Processing*, 131, 105872.
- Fan, L., Liang, G., Zhang, C., Fan, L., Yan, W., Guo, Y., Dong, C. (2021). Visible-light-driven photoelectrochemical sensing platform based on BiOI nanoflowers/TiO₂ nanotubes for detection of atrazine in environmental samples. *Journal of Hazardous Materials*, 409, 124894.



- Gao, H., Shangguan, W., Hu, G., & Zhu, K. (2016). Preparation and photocatalytic performance of transparent titania film from monolayer titania quantum dots. *Applied Catalysis B: Environmental*, 180, 416–423.
- Gnida, P., Jarka, P., Chulkin, P., Drygała, A., Libera, M., Tański, T., & Schab-Balcerzak, E. (2021). Impact of TiO₂ nanostructures on dye-sensitized solar cells performance. *Materials*, 14(7), 1633.
- Gong, D., Grimes, C.A., Varghese, O.K., Hu, W., Singh, R.S., Chen, Z., Dickey, E.C., & Mater, J. (2001). *Res*, 16, 3331.
- Hui, F.Z., Chang, J.L., Yue, K.I., Sun, L., & Li, J. (2007). Some critical structure factors of titanium oxide nanotubes arrays in its photocatalytic activity. *Environ. Sci. Technol*, 41, 4735-4740.
- Ji, L., Zhang, Y., Miao, S., Gong, M., & Liu, X. (2017). In situ synthesis of carbon doped TiO₂ nanotubes with an enhanced photocatalytic performance under UV and visible light. *Carbon*, 125, 544–550.
- Kaewwongsa, S. (2017). Preparation and characterization of CrZrN thin films deposited by reactive dc magnetron co - sputtering, *Burapha University*.(in thai)
- Kang, X., Liu, S., Dai, Z., He, Y., Song, X., & Tan, Z. (2019). Titanium dioxide: from engineering to applications. *Catalysts*, 9(2), 191.
- Liang, H., & Li, X. (2009). Effects of structure of anodic TiO₂ nanotube arrays on photocatalytic activity for the degradation of 2,3-dichlorophenol in aqueous solution. *Journal of Hazardous Materials*, 162 (2-3), 1415–1422.
- Lim, S.L., Liu, Y., Li, J., Kang, E.-T., & Ong, C.K. (2011). Transparent titania nanotubes of micrometer length prepared by anodization of titanium thin film deposited on ITO. *Applied Surface Science*, 257 (15), 6612–6617.



- Lv, H., Li, N., Zhang, H., Tian, Y., Zhang, H., Zhang, X., & Li, Y. (2016). Transferable TiO₂ nanotubes membranes formed via anodization and their application in transparent electrochromism. *Solar Energy Materials and Solar Cells*, 150, 57–64.
- Lee, T., Lee, W., Kim, S., Lee, C., Cho, K., Kim, C., & Yoon, J. (2021). High chlorine evolution performance of electrochemically reduced TiO₂ nanotube array coated with a thin RuO₂ layer by the self-synthetic method. *RSC Advances*, 11(20), 12107–12116.
- Matus, Z., Stepan, K., Radim, C., Sarka, P., Hana, K., Jan, T., Zdenek, H., Yalavarthi, R., Josef, K., Alberto, N., Patrik, S., Radek, Z. (2018). TiO₂ nanotubes on transparent substrates: control of film microstructure and photoelectrochemical water splitting performance. *Catalysts*, 8(1), 25.
- Naduvath, J., Bhargava, P., & Mallick, S. (2015). Mechanism of titania nanograss formation during anodization, 626, 15 -19.
- Nguyen, H. H., Gyawali, G., Martinez-Oviedo, A., Kshetri, Y. K., & Lee, S. W. (2020). Physicochemical properties of Cr-doped TiO₂ nanotubes and their application in dye-sensitized solar cells. *Journal of Photochemistry and Photobiology A: Chemistry*, 397, 112514.
- Perillo, P. M., & Rodríguez, D. F. (2021). Photocatalysis of methyl orange using free standing TiO₂ nanotubes under solar light. *Environmental Nanotechnology, Monitoring & Management*, 16, 100479.
- Richter, C., & Schmuttenmaer, C.A. (2010). Exciton-like trap states limit electron mobility in TiO₂ nanotubes. *Nature Nanotechnology*, 5 (11), 769–772.
- Regonini, D., Satka, A., Jaroenworarluck, A., Allsopp, D.W.E., Bowen, C.R., & Stevens, R. (2012). Factors influencing surface morphology of anodized TiO₂ nanotubes. *Electrochimica Acta*, 74, 244–253.
- Swinehart, D.F. (1962). The Beer-Lambert Law. *Journal of Chemical Education*, 39 (7), 333.



- Srimuangmak, K., & Niyomwas, S. (2011). Effects of voltage and addition of water on photocatalytic activity of TiO₂ nanotubes prepared by anodization method. *Energy Procedia*, 9, 435 - 439.
- Simi, V.S., & Rajendran, N. (2017). Influence of tunable diameter on the electrochemical behavior and antibacterial activity of titania nanotubes arrays for biomedical applications. *Materials Characterization*, 129, 67-79.
- Sreekantan, S., & et al. (2009). Influence of electrolyte pH on TiO₂ nanotube formation by Ti anodization. *Journal of Alloys and Compounds*, 485 (1–2), 478-483.
- Suhaimy, S.M., Lai, C., Tajuddin, H., Samsudin, E., & Johan, M. (2018). Impact of TiO₂ nanotubes' morphology on the photocatalytic degradation of simazine pollutant. *Materials*, 11 (11), 2066.
- Szkoda, M., Lisowska, A., Grochowska, K., Skowronski, L., Karczewski, J., & Siuzdak, K. (2016). Semi – transparent ordered TiO₂ nanostructures prepared by anodization of titanium thin films deposited onto the FTO substrate. *Applied Surface Science*, 381, 36-41.
- Thomas, F., Thomas, C., Valérie, K., My Ali, E.K. (2020). Comparative study of the photocatalytic effects of pulsed laser deposited CoO and NiO nanoparticles onto TiO₂ nanotubes for the photoelectrochemical water splitting. *Solar Energy Materials and Solar Cells*, 217, 110703.
- Vera, M.L., Avalos, M.C., Rosenberger, M.R., Bolmaro, R.E., Schvezov, C.E., & Ares, A.E. (2017). Evaluation of the influence of texture and microstructure of titanium substrates on TiO₂ anodic coatings at 60 V, 131, 348-358.
- Wang, X., Li, Z., Xu, W., Kulkarni, S.A., Batabyal, S.K., Zhang, S., & Wong, L.H. (2015). TiO₂ nanotube arrays based flexible perovskite solar cells with transparent carbon nanotube electrode. *Nano Energy*, 11, 728–735.



- Xu, C., Rangaiah, G.P., & Zhao, X.S. (2014). Photocatalytic degradation of methylene blue by titanium dioxide: experimental and modeling study. *Industrial & Engineering Chemistry Research*, 53 (38), 14641-14649.
- Yang, D.J., Kim, H.G., Cho, S.J., & Choi, W.Y. (2008). *IEEE Trans. Nanotechnol*, 7, 131.
- Yang, P., & et al. (2016). Influence of H₂O₂ and H₂O content on anodizing current and morphology evolution of anodic TiO₂ nanotubes. *Materials Research Bulletin*, 83, 581-589.
- Yuan, L., Wang, C., Cai, R., Wang, Y., Zhou, & G. (2013). Spontaneous ZnO nanowire formation during oxidation of Cu-Zn alloy. *Journal of Applied Physics.*, 114, 023512.
- Zhang, W., Li, H., Hopmann, E., & Elezzabi, A. Y. (2020). Nanostructured inorganic electrochromic materials for light applications. *Nanophotonics*, 10(2), 825–850.